Colloid Journal, Vol. 67, No. 6, 2005, pp. 774–787. Translated from Kolloidnyi Zhurnal, Vol. 67, No. 6, 2005, pp. 850–864.
Original Russian Text Copyright © 2005 by Shchekin, Borisov.

Thermodynamics of Nucleation on the Particles of Salts–Strong Electrolytes: The Allowance for Ion Adsorption in the Droplet Surface Layer

A. K. Shchekin and V. V. Borisov

Fock Institute of Physics, St. Petersburg State University, ul. Ul'yanovskaya 1, Petrodvorets, St. Petersburg, 198504 Russia

Received March 30, 2005

Abstract—The contributions dependent on ionic specificity (including those related to the differences in polarizabilities of cations and anions) to the surface tension and ion adsorption on the boundary between an aqueous strong electrolyte solution and the vapor–gas phase are taken into account. The role of these contributions in the thermodynamics of vapor condensation on salt particles completely dissolved in droplets that are emerged on these particles from the vapor is studied. Consistent domains of the applicability of the analytical theory suggesting the complete dissolution of a salt particle and the dissociation of substance comprising this particle into ions, as well as the ideal behavior of solution in a droplet and the linearization with respect to excess electric potentials near the droplet surface, are established in the approximation of a quasi-planar interface. Formulas are derived for the threshold values of the chemical potential of vapor molecules upon the barrierless condensation and for critical vapor supersaturations upon the barrier condensation on salt particles. In the explicit form, these formulas express the dependence of these values on the initial size of salt particles, physicochemical parameters of solution in droplets, and the charge of formed ions. Calculations for water condensation on NaCl, Na_2SO_4, and $MgCl_2$ particles are performed using these formulas.

INTRODUCTION

Solid particles composed of inorganic salts (e.g., NaCl, Na_2SO_4, and $(NH_4)_2SO_4$) are widespread nuclei of water vapor condensation in Earth's atmosphere. It is known that, due to a high solubility in water droplets condensing from surrounding vapor–gas medium, these condensation nuclei become the sites of intense nucleation of droplets in water vapor even at very low vapor supersaturations. In the thermodynamics of nucleation on salt particles completely dissolved in emerging droplets whose basis was laid by Kohler [1], the adsorption of ions of a dissolved substance comprising the particle in the surface layer of emerging droplets is usually ignored [2, 3]. However, there is still no answer in the published literature as to the question when this disregard is justified and when the adsorption of ions should be taken into account. In addition, within the framework of Kohler's theory, different salts almost equally affect threshold vapor supersaturations corresponding to the onset of barrierless nucleation, provided that the degrees of their dissociation in solution and initial sizes of nuclei set by the number of salt molecules coincide. The differences in critical vapor supersaturations observed in experiment upon intense condensation on particles from readily dissolved salts of different ion compositions were explained [3, 4] by introducing the degree of dissociation dependent on the sort of ions and salt concentration in a solution.

It could be expected that it is the adsorption of ions coming from dissolving condensation nucleus on the droplet surface that is responsible for the specific effect of salt forming this nucleus on the process of droplet emergence. The allowance for the ion adsorption in the thermodynamic description of droplet emergence on soluble condensation nuclei of strong electrolyte implies seemingly the allowance for the change in the surface tension of droplets in the presence of dissolved electrolyte. In this case, in view of the finite sizes of condensation nucleus and droplet, one should also take into account the balance of dissolved substance comprising condensation nucleus between the volume and surface layer of a droplet.

As far back as the beginning of last century, it was known that the dissolution of the majority of inorganic salts in water results in an increase in the surface tension of a solution. The theory of the surface tension of strong electrolyte solutions for the case of solution–gas planar interface was first developed by Wagner [5] and then elaborated by Onsager and Samaras [6]. Later, Buff and Stillinger [7], using the method of integral equations, confirmed Onsager and Samaras' results; at the end of the 1990s, these results were generalized by Groenewald [8] to the case of curved interfaces. Recently, Levin [9] compared the Onsager–Samaras formula for the surface tension of electrolyte solutions with analogous relations derived within the framework of canonic and grand canonic ensembles and demon-

1061-933X/05/6706-0774 © 2005 Pleiades Publishing, Inc.

strated that this formula presents correct asymptotic at low solution concentrations.

The Onsager–Samaras theory takes into account only the forces of repulsion of an ion in the solution from the interface caused by the "image forces" for a point charge in the vicinity of flat boundary between two dielectrics. Since the value of image forces is proportional to the square of ion charge and in the principal order does not depend on other ion characteristics, the Onsager–Samaras theory predicts equal surface tensions for aqueous solutions of any symmetric 1 : 1 electrolyte of a given concentration and equal contributions of cations and anions to adsorption. This statement is not confirmed in practice upon measuring the surface tension of electrolyte solutions within a rather wide concentration range [10–12].

In [13–15], it was proposed to modify the Onsager–Samaras theory and take into account, in addition to image forces, van der Waals (vdW) forces arising due to ion polarization. The character (attraction or repulsion) and the value of these forces are determined by the ion polarizability. The contribution to surface tension due to vdW forces turned out to be dependent on the ion nature and comparable (by the order of magnitude) with the contribution related to the image forces for the point charge. Thus, the approach proposed in [13–15] could dispose of the shortcomings of the Onsager–Samaras theory associated with the disregard for the specificity of electrolyte ions, while retaining at the same time the main ideas of this theory. The development of this approach as applied to the diversity of problems of the theory of surface phenomena involving the specificity of ions of dissolved electrolytes has been considered in recent works [16–18].

In recent years, extensive joint studies of the molecular structure at the aqueous electrolyte solution–air interface by the methods of molecular dynamics, quantum chemistry, and the spectroscopy of surface vibrational states have been performed [19–22]. These studies demonstrated that differences in polarizability, charge magnitude, and ion size profoundly affect the charge distribution and profile of electric potential in the solution surface layer. Whereas cations and doubly charged anions of inorganic salts are effectively repulsed from the solution surface, single-charged anions tend to the accumulation in the surface layer; moreover, their adsorption increases with the polarizability of anions.

The main aim of this paper is to allow for the effect of contributions ions to the surface tension of strong electrolyte solution and the adsorption of solute ions in the solution surface layer. We will investigate the role of these contributions in the thermodynamics of heterogeneous nucleation on soluble condensation nuclei from salts – arising due to specificity of strong electrolytes. The prime attention will be focused on the elucidation of the consistent domains of applicability of the analytical theory of heterogeneous nucleation suggesting the complete dissolution of condensation nucleus and the ideality of solution in the droplet, linearization with respect to excess electric potentials, and the approximation of quasi-planar interface. As a result, we derive formulas for the threshold value of the chemical potential of vapor molecules upon the barrierless nucleation and for critical vapor supersaturations upon the barrier nucleation on condensation nuclei composed of solid particles of inorganic salts. These formulas explicitly express the dependence of threshold and critical vapor supersaturations on the initial size of condensation nuclei, charge magnitude, and physical parameters of ions formed during the dissolution. The results will be illustrated by the numerical calculations of the profiles of electric potentials and ion concentrations in the vicinity of solution–vapor interface, as well as by the calculations (using the derived formulas) of threshold and critical supersaturations of water vapor upon the condensation of one-component salt particles in three different cases when these particles consist of NaCl, Na_2SO_4, and $MgCl_2$.

1. SURFACE TENSION AND ADSORPTION ON ELECTROLYTE SOLUTION–GAS PLANAR INTERFACE

Following the Onsager–Samaras theory [6], we denote by $w_i(\xi)$ the excess (compared to the ion energy in the bulk of electrolyte solution) energy of the ion of ith kind located at distance ξ from the solution–gas planar interface. We assume that the $w_i(\xi)$ energy decreases according to the power or exponential law with an increase in distance from the interface so that $w_i(\xi) \longrightarrow 0$ at $\xi \longrightarrow \infty 0$. At the thermodynamic equilibrium of solution, the ion concentration near the interface differs from that in the bulk solution by factor $\exp(-w_i/k_BT)$, where k_B is Boltzmann's constant, and T is the absolute temperature. Then, adsorption Γ_i of ith ions can be represented as

$$\Gamma_i = \frac{x_i}{v}\int_0^\infty \left[\exp\left(-\frac{w_i(\xi)}{k_BT}\right) - 1\right] d\xi. \qquad (1.1)$$

Here, x_i is the relative molecular concentration of i th component of solute (the number of ith ions per solvent molecule) in the bulk phase of solution and v is the molecular volume of solvent, which can be considered as constant at relatively low concentrations x_i. The integration with respect to coordinate ξ in Eq. (1.1) is formally performed from zero to infinity, although the lower limit cannot be smaller than ion diameter (upon the ion hydration) and the integrand is practically nullified at higher (albeit finite) ξ values.

At constant temperature and under the assumption of the complete dissociation of electrolyte molecules, the Gibbs adsorption equation for equimolecular surface with respect to solvent has the following form:

$$d\sigma = -\sum_i \Gamma_i d\mu_i', \tag{1.2}$$

where σ is the surface tension of electrolyte solution and μ_i' is the chemical potential of ith ions. For ideal electrolyte solutions, $d\mu_i' = k_B T d\ln x_i$; hence, allowing for Eq. (1.1), we have

$$d\sigma = -\frac{k_B T}{v}\sum_i dx_i \int_0^\infty \left[\exp\left(-\frac{w_i(\xi)}{k_B T}\right) - 1\right] d\xi. \tag{1.3}$$

Excess energy w_i is constituted from several contributions [14–18]

$$w_i(\xi) = ez_i\varphi(\xi) + \frac{(\varepsilon-1)}{\varepsilon(\varepsilon+1)}\frac{e^2 z_i^2}{4\xi}e^{-2\kappa\xi} + \frac{H_i}{\xi^3} + \Delta V_i(\xi). \tag{1.4}$$

The first term in the right-hand side of Eq. (1.4) considers changes in electric field potential $\varphi(\xi)$ caused by the presence of interface and created in point ξ by all other ions in solution. Here, e is the value of elementary electric charge and z_i is the valence of ith ion. The second term is related to the image force acting on the ion in the solution with permittivity ε near the boundary with the gas medium with the permittivity equals unity. Factor $e^{-2\kappa\xi}$ considers Debye's screening due to the planar stratification of ions with different signs in the vicinity of solution–gas interface and κ is the reciprocal Debye length determined by relation

$$\kappa^2 = \frac{4\pi e^2}{k_B T \varepsilon v}\sum_i x_i z_i^2 \tag{1.5}$$

(permittivities in the bulk part of solution and in the surface layer are assumed to be equal). The third term in the right-hand side of Eq. (1.4) is the vdW energy due to ion polarization (without allowance for electromagnetic retardation); H_i is the Hamaker constant for ith ion (see [14–18]). The last term in the right-hand side of Eq. (1.4) allows for the change in the hydration energy of ith ion due to the deviation of the surface profile of a solvent density from its bulk value; $\Delta V_i(\xi)$ decreases no slower than $1/\xi^3$. Note that macroscopic expressions for the second and third contributions to excess energy (1.4) are applicable only at some distance from the interface that is no shorter than effective diameters of ions. It is seen that excess energy $w_i(\xi)$ has the meaning of the minimal work needed to transfer ith ion from the bulk of solution to distance ξ from the solution–gas interface. Therefore, chemical potential $\tilde{\mu}_i'$ of ith component of a solute at distance ξ from the interface can be written as $\tilde{\mu}_i' - \mu_i' = k_B T \ln(\tilde{x}_i(\xi)/x_i) + w_i(\xi)$, where $\tilde{x}_i(\xi)$ denotes the local concentration of ith ions at distance ξ from the interface. It is evident that in equilibrium solution, $\tilde{\mu}_i' = \mu_i'$.

Note that, already at distances $\xi > 10$ Å, approximate equality

$$\exp\left(-\frac{w_i(\xi)}{k_B T}\right) \approx 1 - \frac{w_i(\xi)}{k_B T}$$

is fulfilled with good accuracy.

Then, integral with respect to ξ in Eqs. (1.1) and (1.3) can be divided into two parts

$$\int_0^\infty \left[\exp\left(-\frac{w_i(\xi)}{k_B T}\right) - 1\right] d\xi = D_i - \int_d^\infty \frac{w_i(\xi)}{k_B T} d\xi, \tag{1.6}$$

where d is the distance from the interface equals several effective ion diameters. In the range of moderately low and high concentrations, parameters

$$D_i \equiv \int_0^d \left[\exp\left(-\frac{w_i(\xi)}{k_B T}\right) - 1\right] d\xi \tag{1.7}$$

should be slightly dependent on x_i. In the range of very low solution concentrations, the dependence of the reciprocal Debye length κ on x_i turned out to be significant; in view of relations (1.4) and (1.7), this dependence can cause changes in the D_i values. However, this range is very narrow, and hereafter, we assume that the D_i values to be parameters independent of concentrations x_i. To verify this assumption (and for the direct calculation of parameters D_i), it is necessary to find the profile of potential $\varphi(\xi)$; corresponding problem will be discussed in Section 2.

In view of Eq. (1.4), the contribution of potential $\varphi(\xi)$ to Eq. (1.3) from the second term in Eq. (1.6) is equal to zero due to solution electroneutrality. Integrating Eq. (1.3) with allowance for relations (1.4) and (1.6), in the principal approximation with respect to $\kappa d \ll 1$, we arrive at

$$d\sigma = \frac{(\varepsilon-1)e^2}{4\varepsilon(\varepsilon+1)v}\sum_i \left(\ln\frac{1}{2\kappa d} - \gamma_E\right) d(z_i^2 x_i) - \frac{1}{v}\sum_i \left(k_B T D_i - \frac{H_i}{2d^2}\right) dx_i, \tag{1.8}$$

where $\gamma_E = 0.5772\ldots$ is Euler's constant; hydration contribution $\Delta V_i(\xi)$ is ignored upon the integration of the second term in the right-hand side of Eq. (1.6). Condition $\kappa d \ll 1$ restricts the solution concentration from the upper bound stronger than the condition of solution ideality.

The first term of expression in the right-hand side of Eq. (1.8) with allowance for Eq. (1.5) represents exact differential. Integrating Eq. (1.8) along line segment $(x_i)_t = x_i t$, $0 \le t \le 1$, and considering that the values of H_i and D_i are independent of concentration x_i, we obtain

$$\sigma - \bar{\sigma} = \frac{(\varepsilon - 1)e^2}{8\varepsilon(\varepsilon + 1)v}\sum_i x_i z_i^2 \times\left[1 - \ln\left(\frac{16\pi e^2}{k_B T\varepsilon v}d^2\sum_j x_j z_j^2\right) - 2\gamma_E\right] - \sum_i\left(k_B T\frac{D_i}{v} - \frac{H_i}{2vd^2}\right)x_i, \quad (1.9)$$

where $\bar{\sigma}$ is the surface tension of pure solvent. For total adsorption Γ of ions of all types in the surface layer, from Eq. (1.1) with allowance for Eqs. (1.4) and (1.6) and condition of electroneutrality, we have

$$\Gamma = \sum_i \Gamma_i = \frac{(\varepsilon - 1)e^2}{8k_B T\varepsilon(\varepsilon + 1)v} \times\sum_i x_i z_i^2\left[\ln\left(\frac{16\pi e^2 d^2}{k_B T\varepsilon v}\sum_j x_j z_j^2\right) + 2\gamma_E\right] + \frac{1}{v}\sum_i\left(D_i - \frac{H_i}{2k_B T d^2}\right)x_i. \quad (1.10)$$

At $H_i = 0$, formulas (1.9) and (1.10) in the limit of low solution concentrations for 1 : 1 electrolyte are consistent with limiting asymptotics of the Onsager–Samaras theory for the surface tension and adsorption [6] written in our notation as

$$\sigma - \bar{\sigma} = -\frac{k_B T}{16\pi\kappa^2}\left[\frac{3}{2} - \ln(\kappa e^2/2\varepsilon k_B T) - 2\gamma_E\right],$$
$$\Gamma = \frac{\kappa^2}{64\pi}[\ln(\kappa e^2/2\varepsilon k_B T) + 2\gamma_E - 1] \quad (1.11)$$

(exact transition from Eqs. (1.9) and (1.10) to (1.11) requires the integration of Eq. (1.7) at $H_i = 0$, $\varphi(\xi) = 0$, and $\Delta V_i(\xi) = 0$).

Hereafter, instead of the σ and Γ values, it is more convenient to use dimensionless surface tension a and adsorption s

$$a \equiv (36\pi v^2)^{1/3}\sigma/k_B T, \quad s \equiv (36\pi v^2)^{1/3}\Gamma. \quad (1.12)$$

Introducing dimensionless coefficients

$$A \equiv \frac{(36\pi)^{1/3}}{k_B T}\frac{(\varepsilon - 1)e^2}{8\varepsilon(\varepsilon + 1)v^{1/3}},$$
$$B_i \equiv \frac{16\pi e^2}{k_B T\varepsilon v}d^2 \times\exp\left[\frac{8\varepsilon(\varepsilon + 1)}{(\varepsilon - 1)e^2 z_i^2}\left(k_B T D_i - \frac{H_i}{2d^2}\right) + 2\gamma_E\right], \quad (1.13)$$

from Eqs. (1.9) and (1.10) with allowance for Eq. (1.12), we obtain

$$a = \bar{a} + A\sum_i x_i z_i^2\left[1 - \ln\left(B_i\sum_j x_j z_j^2\right)\right], \quad (1.14)$$

$$s = A\sum_i x_i z_i^2 \ln\left(B_i\sum_j x_j z_j^2\right), \quad (1.15)$$

where $\bar{a}$ is the dimensionless surface tension of pure solvent. In particular, for the general case of asymmetric electrolyte dissociating in solution into ions with charges $z_1 e$ and $-|z_2|e$, we find

$$a = \bar{a} + \tilde{A}x[1 - \ln(\tilde{B}x)], \quad (1.16)$$

$$s = \tilde{A}x\ln(\tilde{B}x), \quad (1.17)$$

where x is the total ion concentration, and

$$\tilde{A} \equiv z_1|z_2|A, \quad \tilde{B} \equiv z_1|z_2|(B_1^{z_1}B_2^{|z_2|})^{\frac{1}{z_1 + |z_2|}}. \quad (1.18)$$

2. ALLOWANCE FOR THE SPECIFICITY OF IONS IN CALCULATIONS OF SURFACE TENSION AND ADSORPTION

As is seen from formulas (1.9) and (1.10), the dependence of surface tension and adsorption on the solution surface on the nature of dissolved salt should be manifested via the D_i and H_i values and is due to the allowance for both vdW forces and hydration contributions to excess energy w_i of adsorbing ions and ion sign-dependent contribution to Eq. (1.6) from self-consistent electric potential $\varphi(\xi)$ in view of Eq. (1.4). The specificity of various soluble salts in the process of heterogeneous nucleation can be revealed via such an effect on the surface tension and adsorption of ions in the surface layer of droplets of aqueous solutions nucleating on the condensation nuclei composed of these salts.

Let us consider in more detail the behavior of parameters D_i depending on the kind of ions and their concentration. For this purpose, we turn to the numerical solution of the Poisson–Boltzmann equation for self-consistent potential $\varphi(\xi)$. Because in the subsequent sections, we will need only experimentally determined dimensionless coefficients $\tilde{B}$ (which, according to Eq. (1.18) include D_i and H_i) to illustrate the behavior of parameters D_i, in this section we confine ourselves to the case of symmetric 1 : 1 electrolyte solution and set $\Delta V_i(\xi) = 0$. Instead of subscripts "i," we use "+" and "–" designations for the values referring to positive and negative ions, respectively. Then, local concentration $\tilde{x}_\pm(\xi)$ of cations and anions at a distance of ξ from the solution–air interface, in view of what have been said in section 1, is written as

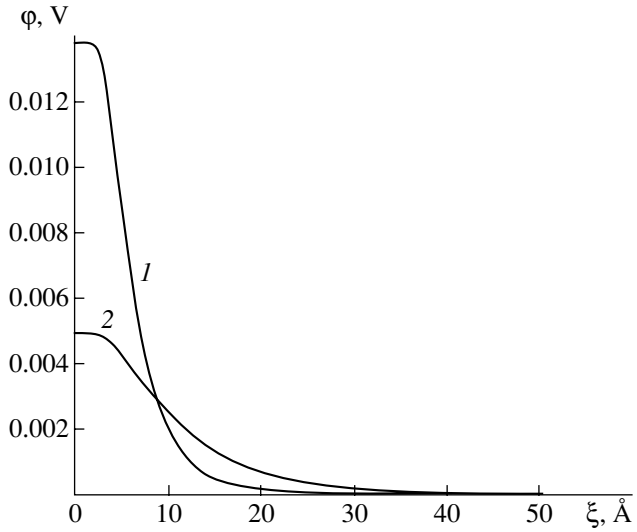


Fig. 1. Dependences of self-consistent surface potential φ on the distance from the solution–air interface for aqueous NaCl solutions with concentration of (*1*) 1 and (*2*) 0.1 mol/l.

$$\tilde{x}_{\pm}(\xi) = (x/2)e^{-w_{\pm}(\xi)/k_BT}. \quad (2.1)$$

Correspondingly, the Poisson–Boltzmann equation for potential φ(ξ) has the form

$$\frac{d^2\varphi(\xi)}{d\xi^2} = -\frac{4\pi e}{\varepsilon v}(\tilde{x}_+(\xi) - \tilde{x}_-(\xi)). \quad (2.2)$$

Taking into account that potential φ decays in the depth of solution, we write

$$\varphi(\xi) \xrightarrow[\xi\to\infty]{} 0, \quad d\varphi/d\xi \xrightarrow[\xi\to\infty]{} 0. \quad (2.3)$$

Also considering that the solution to this equation should ensure the total electroneutrality

$$\int_0^\infty (\tilde{x}_+(\xi) - \tilde{x}_-(\xi))d\xi = 0,$$

that, with allowance for Eq. (2.2) and the second of conditions (2.3), requires equality

$$d\varphi/d\xi|_{\xi=0} = 0. \quad (2.4)$$

During the numerical solution of Eq. (2.2), the value of potential φ at the interface (at ξ = 0) is chosen such that condition (2.3) should be fulfilled.

As was mentioned above, expression (1.4) for excess energy $w_{\pm}(\xi)$ of positive and negative ions is valid only at some distances $\delta_{\pm}$ from the phase boundaries that are typical of each kind of ions and coincide (by the order of magnitude) with the size of corresponding ion. Let us assume that $\exp(-w_{\pm}(\xi)/k_BT)$ vanishes at $0 \le \xi \le \delta_{\pm}$ that corresponds to the condition of impermeability of phase boundaries for ions. Values $\delta_{\pm}$ are the adjustment parameters of a problem.

Let us show the results of the numerical solution of Eq. (2.2) for aqueous NaCl solution. We choose values $\delta_+ = 2.2$ Å for Na^+ ion and $\delta_- = 2.5$ Å for Cl^- ion as parameter $\delta_{\pm}$. According to [15], the Hamaker constant of *i*th ion is determined by relation

$$H_i \approx (n^2 - n_{air}^2)\alpha_i^*(0)\frac{h\omega_i}{2\pi}, \quad (2.5)$$

where n and n_{air} are the refractive indices of water and air, respectively; $h\omega_i/2\pi$ is the electron affinity for the ion (h is Planck's constant, ω_i is a certain characteristic frequency of *i*th ion corresponding to the boundary of ultraviolet absorption), and $\alpha_i^*(0)$ is the excess static polarizability of *i* th ion in water determined as a difference between polarizabilities of ion and the same volume of water. Thus, positive values of the Hamaker constant correspond to the ions with higher (than water) polarizability. Correspondingly, such ions enhance the effect of the surface inactivity of the solute typical of the Onsager–Samaras approximation with no allowance for ion polarizability. The reverse situation is possible, when the polarizability of ions turned out to be lower than that of water molecules [15]. In accordance with [15], upon the calculation of potential φ, we determined Hamaker constants for sodium and chlorine ions as $H_+ = -1 \times 10^{-50}$ J m^3 and $H_- = 31 \times 10^{-50}$ J m^3, respectively.

Figure 1 shows the dependences of potential φ on distance ξ to the solution–air interface illustrated by the curves corresponding to the total ion concentrations x = 0.036 (curve *1*) and x = 0.0036 (*2*). The potential corresponding to less concentrated solution is characterized by smaller initial value; however, this solution corresponds to larger Debye length, in view of this fact, the potential decreases slower with distance and, in a wide distance range, it appeared to be larger than the potential of more concentrated solution. Note that, at solution temperature T = 300 K, the energy of 0.01 eV is equal to $0.39k_BT$. Correspondingly, it is clear from Fig. 1, that the contribution of potential φ to ion excess energy $w_{\pm}(\xi)$ at distance ξ < 10 Å from the interface is comparable with k_BT and the linearization of this contribution to $\exp(-w_{\pm}(\xi)/k_BT)$ is justifiable only at ξ > 10 Å, as was mentioned in Section 1.

Figure 2 presents the dependences of local concentrations $\tilde{x}_{\pm}(\xi)$ of Na^+ (curve *1*) and Cl^- (curve *2*) ions in a NaCl solution on distance ξ from the interface. Concentrations $\tilde{x}_{\pm}(\xi)$ of positive and negative ions are expressed in units of their total concentration $x/2$ and, according to Eq. (2.1), correspond to the profile of potential φ(ξ) in a solution with the bulk concentration of 1 mol/l (x = 0.036) shown in Fig. 1. It is seen that nonuniform charge distribution arises in the solution surface layer: fairly thin layer with dominant positive charge (i.e., Na^+ ions) is located near the interface; the prevalence of negative charge (i.e., Cl^- ions) is

observed at large distances. The surface concentration of positive ions rises rather slowly; at a distance of above 20 Å from the interface, it still remains lower than the bulk concentration of these ions.

Note that the problem of the numerical solution of self-consistent potential φ in the vicinity of gas–electrolyte solution interface was repeatedly discussed with allowance for contributions that are additional to the potential of image forces (e.g., see [15–17]). The potential profile obtained in [15] when considering the role of vdW forces related to the ion polarization slightly differs from that shown in Fig. 1, because significant condition (2.4) is not fulfilled for the profile reported in [15]. However, the potential calculated in [15] has the same sign as the potential calculated in this section and qualitatively describes the same space charge distribution. The specific adsorption of anions at the solution–air interface was phenomenologically taken into account in [16, 17]. The potential calculated in [16, 17] has different sign. This agrees with the latest results [19–21] where, within the framework of quantum-chemical calculations of the energy of ions in the surface layer of electrolyte solution with allowance for their polarizability and molecular dynamics calculation of the space ion distribution, it was revealed that the Cl^- ions should by located to the interface closer than the Na^+ ions. An analogous result could be obtained, with explicit allowance for the difference between negative hydration contribution $\Delta V_i(\xi)$ for cations and anions by the method considered in this section; however, at present, there is no adequate analytical representation of this contribution.

Regardless of the drawbacks due to the employed approximations, the numerical calculation of potential profile makes it possible to illustrate the dependence of $D_\pm$ values on total concentration x of ions in the solution. These data are shown in Fig. 3. Profiles of potential $\varphi(\xi)$ were found for each concentration; corresponding profiles of excess energy $w_\pm(\xi)$ were calculated using Eq. (1.4), which then were employed to calculate the $D_\pm$ values by Eq. (1.7). Upon calculations, we used two sets of the values of the Hamaker constant: $H_+ = -1 \times 10^{-50}$ J m^3 and $H_- = 31 \times 10^{-50}$ J m^3 taken from [15] (curves *1* and *1'*) and $H_+ = 0.83 \times 10^{-50}$ J m^3 and $H_- = 15 \times 10^{-50}$ J m^3 taken from [17] (curves *2* and *2'*).

It is seen from Fig. 3 that, in both considered cases, the D_+ value corresponding to Na^+ ions (curves *1* and *2*) is negative and slightly dependent on the solution concentration throughout the considered concentration range. Similar D_- value for Cl^- ions (curves *1'* and *2'*) is also negative and notably changes only in the range of very low concentrations that confirms assumptions on the behavior of the $D_\pm$ values made in Section 1.

Note that the error introduced into Eq. (1.9) by the assumption of constant $D_\pm$ values does not exceed 7% of the contribution to σ related to D_i and does not increase with the concentration. Relative error introduced by the assumption of constant $D_\pm$ values into

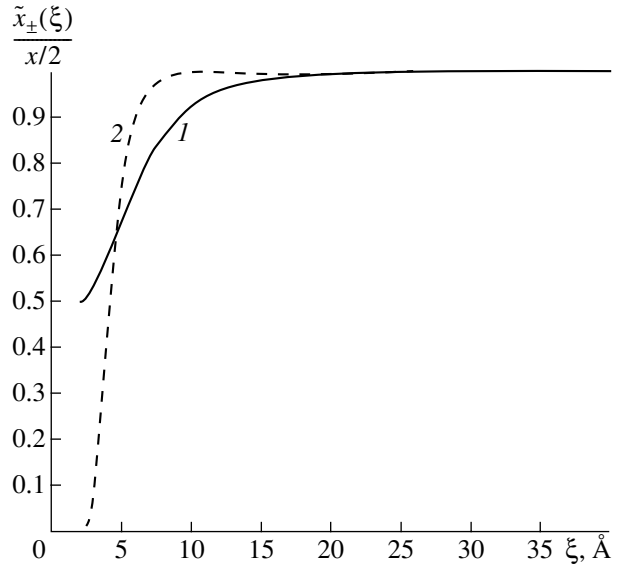


Fig. 2. Dependences of local surface concentrations of (*1*) Na^+ and (*2*) Cl^- ions on the distance from the solution–air interface for aqueous NaCl solutions with concentration of 1 mol/l.

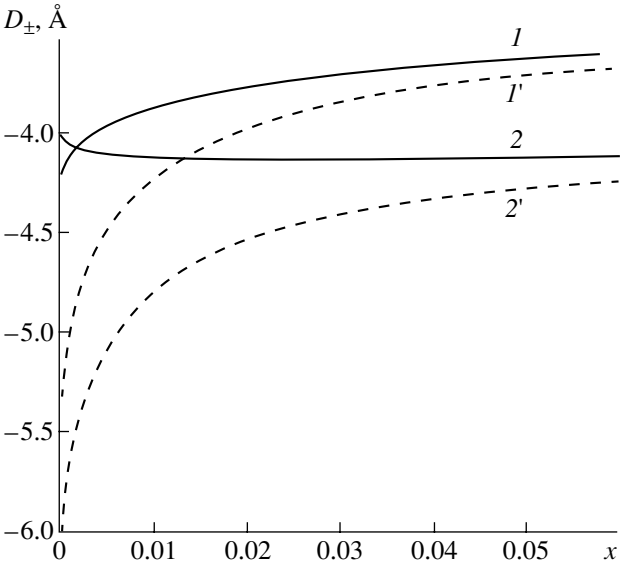


Fig. 3. Dependences of the parameters D_+ (curves *1* and *2* for Na^+ ions) and D_- (curves *1'* and *2'* for Cl^- ions) values on the total solution concentration calculated for two sets of the Hamaker constants (see text).

expression (1.10) for total adsorption Γ of positive and negative ions is also small due to the fact that the $D_\pm$ values enter into this expression as a sum $(D_+ + D_-)$ whose change does not exceed 10%.

3. DETERMINATION OF PARAMETERS $\tilde{B}$ FROM THE DATA ON THE SURFACE TENSION OF AQUEOUS ELECTROLYTE SOLUTIONS

It is seen already from general relations (1.1), (1.3), and (1.4) with allowance for definition (1.5) and, in par-

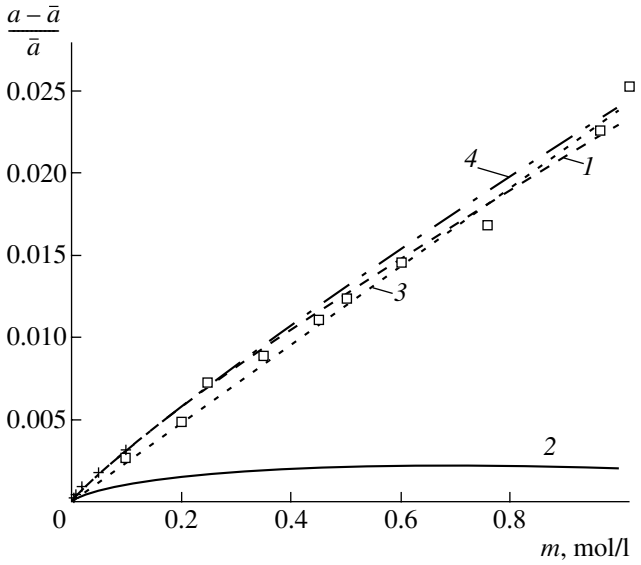


Fig. 4. Dependences of the surface tension of aqueous NaCl solution on the concentration ranged from 0.01 to 1 mol/l (total relative concentration x of ions varies from 0.0036 to 0.036) calculated (*1*) using Eq. (3.6), (*2*) in the Onsager–Samaras approximation, (*3*) in the approximation of Henry adsorption law, and (*4*) by the Schmutzer formula. Crosses and squares denote experimental values taken from [11] and [12], respectively.

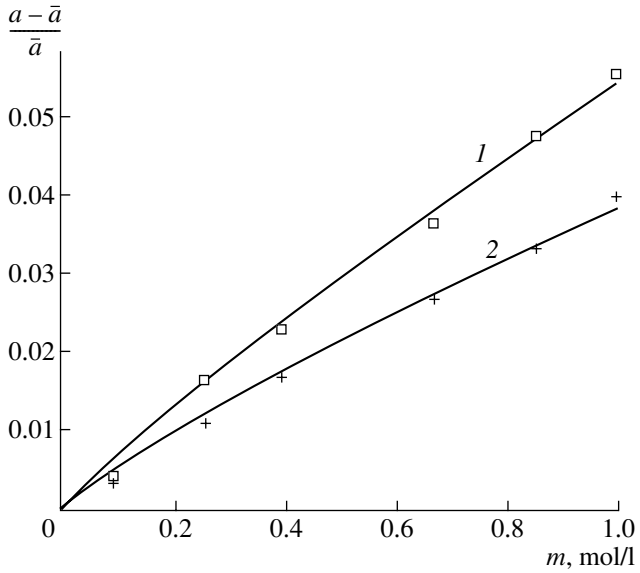


Fig. 5. Dependences of the surface tension of aqueous (*1*) $MgCl_2$ and (*2*) Na_2SO_4 (1 : 2 and 2 : 1 electrolytes, respectively) solutions on the concentration ranged from 0.1 to 1 mol/l (total relative concentration x of ions varies from 0.0036 to 0.036) calculated using Eq. (3.6). Squares denote experimental values for $MgCl_2$ solutions; crosses, for Na_2SO_4 solutions.

ticular from formulas (1.9) and (1.10), that, in the range of low solution concentrations, the main contribution to the correction to the values of surface tension and adsorption is the contribution of the potential of image forces. This contribution is determined only by the ion charges that resulted from the dissociation of dissolved salt and is independent of ion specificity. As the solution concentration increases, the relative contribution of the potential of image forces in the right-hand side of Eq. (1.9) decreases; on the contrary, the relative contribution of the last term describing deviations from the Onsager–Samaras theory increases in proportion to concentration. Therefore, it can be expected that, at fairly high solution concentrations, the linear dependence of the surface tension on concentration becomes dominant.

Let us determine parameters entering into dimensionless equations (1.16) and (1.17). For water as condensate, at $T = 300$ K, we have $\varepsilon = 81$; its dimensional surface tension in the absence of solute, $\bar{\sigma} = 73$ dyne/cm and $v = 3 \times 10^{-23}$ cm^3. Correspondingly, using the first of formulas (1.12), we obtain $\bar{a} = 8.39$; from the first of relations (1.13) for parameter A, $A = 1.34$. Then, in accordance with the first of formulas (1.18) for aqueous solutions of symmetric 1 : 1 and asymmetric 1 : 2 and 2 : 1 electrolytes, we obtain

$$\tilde{A}_{1\text{-}1} = 1.34, \quad \tilde{A}_{1\text{-}2} = \tilde{A}_{2\text{-}1} = 2.68, \qquad (3.1)$$

where subscripts indicate the corresponding type of electrolyte.

Figures 4 and 5 show experimental data [10–12] and calculated curves for the dependence of relative corrections to the value of surface tension of aqueous NaCl solution (symmetric 1 : 1 electrolyte) and aqueous $MgCl_2$ and Na_2SO_4 (asymmetric 1 : 2 and 2 : 1 electrolytes) solutions on the solution concentration expressed in moles per liter. Data for very low [10] (crosses) and low [11, 12] (squares) NaCl solution concentrations are presented in Fig. 4. In addition, the curves corresponding to Henry's law (linear dependence *3* of $a_H = \bar{a} - x/\mathcal{H}$ type, where according to [14], the Hamaker constant $\mathcal{H}$ for aqueous NaCl solution is taken as equal to $\mathcal{H}_{NaCl} = -0.096$), corresponding to the Onsager–Samaras approximation with no allowance for ion polarizability [6] (curve *2* calculated by the first of formulas (1.11)), and to semi-empirical Schmutzer formula [23, 10, 11] combining the Henry law and Onsager–Samaras approximation (curve *4*) are shown in Fig. 4. Curve *1* illustrates the behavior of the relative correction to surface tension corresponding to formula (1.16) with parameters $\tilde{A}_{1\text{-}1} = 1.34$ and $\tilde{B}_{1\text{-}1}$ determined by the least square method using experimental points indicated in Fig. 4.

It is seen from Fig. 4 that the Onsager–Samaras approximation satisfactorily operates at very low salt concentrations; however, as the concentration increases, it becomes increasingly inapplicable. The approximation based on the linear Henry law poorly operates at very low concentrations; however, it satisfactorily describes the range of relatively low concen-

trations. The Schmutzer approximation and Eq. (1.16) give the best results.

Figure 5 demonstrates the dependences of corrections to the surface tension of aqueous $MgCl_2$ and Na_2SO_4 solutions on the solution concentrations. Calculations were performed by formula (1.16) using the second of equalities (3.1) and parameters $\tilde{B}_{2\text{-}1}$ and $\tilde{B}_{2\text{-}1}$ determined by the least square method and experimental points indicated in Fig. 5 [12].

Let us comment in more detail the curves (Figs. 4 and 5) plotted using formula (1.16). It is seen from Figs. 4 and 5 that general approximate formula for the surface tension of electrolyte solution can be written as

$$(a-\bar{a})/\bar{a} = pm\ln(q/m), \tag{3.2}$$

where m is the total solution concentration expressed in moles per liter; p and q are parameters dependent on ion nature. Evidently, m is related to dimensionless concentration x by expression $m = (\rho/M)x$, where ρ is the density of solvent, and M is its molecular mass. For aqueous solutions, we have

$$m = x/0.018. \tag{3.3}$$

Comparing relations (3.2) and (1.16), we see that parameters $\tilde{A}$ and $\tilde{B}$ are related to parameters p and q for aqueous binary solutions via the following expressions:

$$\tilde{A} = 466.11p, \quad \tilde{B} = 151.02/q. \tag{3.4}$$

In accordance with Eq. (3.1), we obtain

$$p_{1\text{-}1} = 0.00287, \quad p_{2\text{-}1} = p_{1\text{-}2} = 0.00574 \tag{3.5}$$

for 1 : 1 and 2 : 1 and 1 : 2 electrolytes, respectively. With allowance for (3.5), according to data shown in Figs. 4 and 5 for aqueous NaCl, Na_2SO_4, and $MgCl_2$ solutions, respectively, we have

$$\begin{aligned}(a_{\mathrm{NaCl}}-\bar{a})/\bar{a} &= 0.00287m\ln(3243.48/m),\\ (a_{\mathrm{Na_2SO_4}}-\bar{a})/\bar{a} &= 0.00574m\ln(845/m),\\ (a_{\mathrm{MgCl_2}}-\bar{a})/\bar{a} &= 0.00574m\ln(13336/m).\end{aligned} \tag{3.6}$$

Passing to the representation of relation for surface tension in the form of Eq. (1.16) with allowance for Eqs. (3.2)–(3.6), we obtain

$$\begin{aligned}a_{\mathrm{NaCl}} &= \bar{a} + 1.34x[1-\ln(0.0467x)],\\ a_{\mathrm{Na_2SO_4}} &= \bar{a} + 2.68x[1-\ln(0.179x)],\\ a_{\mathrm{MgCl_2}} &= \bar{a} + 2.68x[1-\ln(0.0113x)].\end{aligned} \tag{3.7}$$

Experimental data [11, 12] for a large number of symmetric and asymmetric electrolytes demonstrate that relations of type (3.2) (and, correspondingly, with allowance for Eq. (3.4) of type (1.16)) are applicable even at higher solution concentrations than those allowed by inequality $\kappa d \ll 1$. This confirms assumptions on actual independence of D_i values on the concentration made when deriving Eqs. (1.9) and (1.10).

4. INFLUENCE OF THE CURVATURE OF DROPLET SURFACE

Relations (1.16) and (1.17) were derived for the system with planar interface. Let us estimate their applicability for the spherical droplet of electrolyte solution with curvature radius R. The study of the generalization of the Onsager–Samaras theory to the spherical droplets of aqueous electrolyte solutions has been recently performed within the framework of Monte Carlo method [24].

The pattern of the dependence of excess ion energy $w_i(\xi)$ on distance ξ from the interface changes for a spherical surface. Solving the Poisson equation for a single ion positioned in a droplet with permittivity ε along the normal from the spherical boundary of this droplet with the gas phase with permittivity equals unity, it is easy to show that, instead of contribution

$$w_i^{(ifp)}(\xi) = \frac{(\varepsilon-1)}{\varepsilon(\varepsilon+1)}\frac{e^2z_i^2}{4\xi}e^{-2\kappa\xi} \tag{4.1}$$

to expression (1.4) for $w_i(\xi)$, at the planar interface, there appears the contribution to the excess (with respect to the bulk part of a droplet) ion energy related to the image forces, this contribution having the form

$$\begin{aligned}w_i^{(ifs)}(\xi) &= \frac{(\varepsilon-1)}{2\varepsilon R}e^2z_i^2\\ &\times\left(\sum_{l=1}^{\infty}\frac{l+1}{\varepsilon l+l+1}\left(1-\frac{\xi}{R}\right)^{2l}\right)e^{-2\kappa\xi}.\end{aligned} \tag{4.2}$$

In this case, factor $\exp(-2\kappa\xi)$ still describes the Debye screening; however, it occurs only due to the concentration stratification of ions with different signs in the vicinity of spherical solution–gas interface. Performing the summation in Eq. (4.2) with allowance for strong inequality $\varepsilon \gg 1$, as analytical approximation $w_i^{(ifsa)}(\xi)$ for the contribution which is of interest to us, we find

$$\begin{aligned}w_i^{(ifsa)}(\xi) &= \frac{e^2z_i^2}{2R\varepsilon}\left\{\frac{(1-\xi/R)^2}{\xi/R(2-\xi/R)}\right.\\ &\left.-\ln\left[\frac{\xi(2-\xi/R)}{R}\right]\right\}e^{-2\kappa\xi}.\end{aligned} \tag{4.3}$$

Dependences of relations $w_i^{(ifs)}(\xi)/w_i^{(ifp)}(\xi)$ and $w_i^{(ifsa)}(\xi)/w_i^{(ifp)}(\xi)$ on relative distance ξ/R along the normal to droplet boundary calculated by formulas (4.1)–(4.3) are plotted in Fig. 6. At the finite thickness of diffuse electrical layer, the range of ξ/R values considered

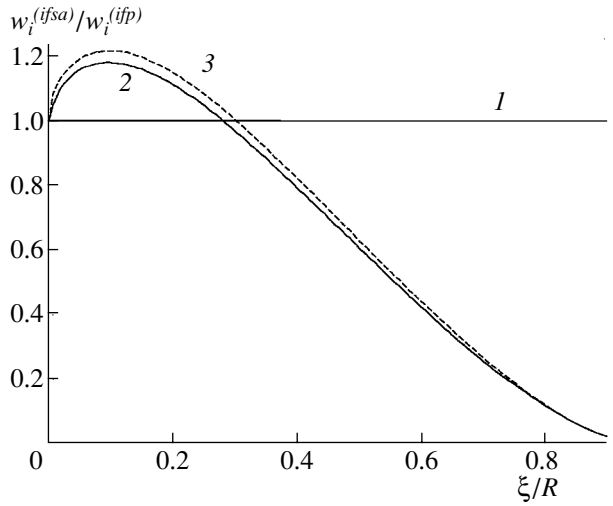


Fig. 6. Dependences of $w_i^{(ifs)}(\xi)/w_i^{(ifp)}(\xi)$ and $w_i^{(ifsa)}(\xi)/w_i^{(ifp)}(\xi)$ on relative distance ξ/R to the interface. Line *1* corresponds to planar boundary; curve *2*, to the $w_i^{(ifs)}(\xi)/w_i^{(ifp)}(\xi)$ ratio calculated by formulas (4.1) and (4.2) for spherical boundary; and curve *3*, to the $w_i^{(ifsa)}(\xi)/w_i^{(ifp)}(\xi)$ ratio calculated by formulas (4.1) and (4.3) for spherical boundary.

in Fig. 6 corresponds to the transition from very large ($\xi/R \approx 0$) to small ($\xi/R \le 1$) droplets. It is seen that the accuracy of analytical approximation (4.3) is fairly high (relative error does not exceed 4%). As will be shown in Section 7, for droplets considered, inequality $R \ge 10\frac{1}{\kappa}$ is fulfilled. In view of Debye screening due to factor $\exp(-2\kappa\xi)$, the contribution to adsorption analogous to the integral in the second term in the right-hand side of Eq. (1.6), for the case of planar interface, is given then only the $\xi/R \le 0.05$ range. As is seen from Fig. 6, the difference between $w_i^{(ifs)}(\xi)$, $w_i^{(ifsa)}(\xi)$, and $w_i^{(ifp)}(\xi)$ in this range of ξ/R values is not too large (less than 15%); hence, with allowance for approximations mentioned above (in particular, when using the linearization of Eq. (1.6)), it will be hereafter ignored.

5. CHEMICAL POTENTIAL OF CONDENSATE IN A DROPLET AND THE HEIGHT OF ACTIVATION BARRIER OF NUCLEATION

Let us now consider the droplet containing ν molecules of condensate (e.g., water). Let the droplet be formed on one-component condensation nucleus (completely dissolved in this droplet) composed of ν_n molecules of inorganic salt whose dissociation in solution resulted in $i\nu_n$ ions (in case of symmetric electrolyte, $i = 2$; in case of asymmetric electrolyte, $i > 2$). For the dilute solution, dimensionless chemical potential b_ν of condensate molecules in a droplet reckoned off from the value at the condensate–vapor planar interface can be written [25, 26] as

$$b_\nu = -x + (2/3)a\nu^{-1/3}, \qquad (5.1)$$

where, as in preceding sections, x is the total relative concentration of all ions in a solution. The first term in the right-hand side of Eq. (5.1) is explained by the osmotic pressure in solution; the second term is due to the capillary pressure under the spherical part of a droplet. Interionic interaction in the bulk part of a droplet is ignored in relation (5.1). The allowance for this interaction would lead to the appearance of positive term in the right-hand side of Eq. (5.1) which is proportional to total concentration x in power of 3/2. In addition, in Eq. (5.1), we ignore the dependence of surface tension a on the surface curvature. As will be shown in the last section, these simplifications suggest the consideration of fairly large droplets. Thus, applying the approach developed in the thermodynamics of nucleation on soluble nuclei, we can use Eq. (1.16) further in Eq. (5.1) and in relevant relations for the dependence of surface tension on the solution concentration at the planar boundary between the liquid and the vapor [25, 26].

Naturally, in the course of formation and growth of condensing droplet on soluble condensation nucleus, the nucleus per se dissolves gradually and the salt solution in a droplet initially cannot be dilute. It was shown [25, 26] that the key role in the thermodynamics of nucleation on soluble nuclei is played by extrema of the chemical potential of condensate in a droplet as a function of its size. In particular, the largest of maxima b_ν is responsible for the threshold values of chemical potential and vapor supersaturation above which the process of nucleation on soluble nuclei proceeds in a barrierless manner. Therefore, upon the construction of the thermodynamics of nucleation, states corresponding to the largest condensate chemical potentials are more important than intermediate states of droplets. If condensate chemical potential reaches the largest maxima in droplets upon the complete nucleus dissolution and low solution concentration, then upon the calculations of the threshold value of vapor supersaturation for barrierless nucleation and critical vapor supersaturations for barrier nucleation (when the states of droplets on the size axis to the right of the coordinate of largest maximum of chemical potential are also important), approximations expressed by formula (5.1) are sufficient. Required conditions for the size and solubility of nucleus will be controlled in Section 7.

The equation of balance of a substance comprising salt particle dissolved in a droplet is represented as

$$x = i\nu_n\nu^{-1} - s\nu^{-1/3}. \qquad (5.2)$$

We consider also that, in this case, the Gibbs adsorption equation, as is seen from Eqs. (1.16) and (1.17), acquires the following form:

$$\partial a/\partial x = -s/x. \quad (5.3)$$

Hereafter, we will be interested in maximum b_ν. Differentiating both parts of Eq. (5.1) with respect to ν with allowance for Eqs. (5.2) and (5.3), using equalities

$$\frac{\partial a}{\partial \nu} = \frac{\partial a}{\partial x}\frac{\partial x}{\partial \nu}, \quad \frac{\partial s}{\partial \nu} = \frac{\partial s}{\partial x}\frac{\partial x}{\partial \nu} \quad (5.4)$$

(followed from the fact that surface tension and adsorption, according to Eqs. (1.16) and (1.17), depend only on concentration x), and passing to the quantity ζ (whose module coincides with the relative fraction of adsorbed substance comprising salt particle at the maximum of chemical potential b_ν at $\nu = \nu_0$) determined as

$$\zeta = s\nu_0^{2/3}/(i\nu_n), \quad (5.5)$$

from the equation for extremum $\partial b_\nu/\partial \nu|_{\nu=\nu_0} = 0$ with allowance for Eqs. (5.1)–(5.4) at $\nu = \nu_0$, we arrive at equation

$$(3-\zeta)^2 - \left(1 - \zeta + \frac{\partial \ln s}{\partial \ln x}\zeta\right)\frac{2a}{s}\zeta = 0. \quad (5.6)$$

Solving Eq. (5.6) as the quadratic equation with respect to ζ, allowing for Eq. (1.17) and the fact that ζ, as well as adsorption s, in case of inorganic salt ions, is a nonpositive value and equal to zero at $s = 0$, we find

$$\zeta = \frac{-(a+3s) + \sqrt{a^2 + 6as + 18as/\ln(\tilde{B}x)}}{2a/\ln(\tilde{B}x) - s}. \quad (5.7)$$

In view of Eqs. (1.16) and (1.17), the explicit solution of Eq. (5.7) determines the dependence of value ζ on total ion concentration x at the maximum of chemical potential. Since relations

$$b_\nu|_{\nu=\nu_0} = (s/\zeta)^{3/2}(i\nu_n)^{-1/2}(2a\zeta/3s + \zeta - 1), \quad (5.8)$$

$$\nu_0 = (s/\zeta)^3(1-\zeta)^3/x^3, \quad (5.9)$$

$$\nu_n = (s/\zeta)^3(1-\zeta)^2/ix^2 \quad (5.10)$$

directly follow from Eqs. (5.1), (5.2), and (5.4), the explicit concentration dependence of quantities $b_\nu|_{\nu=\nu_0}$, ν_0, and ν_n values at the maximum of chemical potential of the condensate in a droplet can be derived using Eq. (5.7). The fact that precisely the maximum of chemical potential is reached at $\nu = \nu_0$, follows from the convex upward pattern of the dependence of b_ν on ν set by relations (5.1) with allowance for Eqs. (1.16) and (1.17). This can be verified also by the sign of the second derivative of b_ν with respect to ν at $\nu = \nu_0$. In fact, relations (5.7)–(5.10), together with Eqs. (1.16) and (1.17), already contain the general solution of the thermodynamic problem of conditions of barrierless nucleation on completely soluble salt condensation nuclei, irrespective of the surface activity of ions formed upon nucleus dissolution.

At the values of vapor chemical potential $b > b_{th} \equiv b_\nu|_{\nu=\nu_0}$ (and, correspondingly, upon vapor supersaturations above the threshold value), the process of droplet nucleation on soluble salt particles does not require the activation energy. The intensity of nucleation at vapor supersaturations below the threshold value is characterized by the height of activation barrier of nucleation. The height of activation barrier is denoted by ΔF and expressed in units of $k_B T$. To determine ΔF, it is sufficient to consider a narrow prethreshold region of vapor metastability lying slightly lower the b_{th} value where vapor chemical potential b can be set as $b = b_{th}(1-\varepsilon)$, where $\varepsilon > 0$ and $\varepsilon \ll 1$ at the macroscopicity of condensation nuclei. Then, for the height of activation barrier ΔF at relative deviation ε from threshold value b_{th}, we arrive at relation [25, 26]

$$\Delta F = \frac{4}{3}\varepsilon^{3/2} b_{th}^{3/2}\left(\frac{2}{|\partial^2 b/\partial \nu^2|_{\nu=\nu_0}}\right)^{1/2}. \quad (5.11)$$

Thus, in order to describe the thermodynamics of barrier and barrierless nucleation of droplets, it is sufficient to know values $b_\nu|_{\nu=\nu_0}$ and $|\partial^2 b_\nu/\partial \nu^2|_{\nu=\nu_0}$ as functions of problem parameters.

In order to find $|\partial^2 b_\nu/\partial \nu^2|_{\nu=\nu_0}$, let us differentiate twice both sides of Eq. (5.1). Taking further into account Eqs. (5.2)–(5.6), we arrive at

$$\begin{aligned}\partial^2 b_\nu/\partial \nu^2|_{\nu=\nu_0} = -\frac{4}{27}\left(\frac{s}{\zeta}\right)^{7/2}\frac{a(i\nu_n)^{-7/2}}{(3-\zeta)^2} \\ \times\left\{(3-\zeta)(3+2\zeta) - 2\frac{a}{s}\zeta^2\right. \\ -2\left(\frac{a}{s}\right)^2\frac{\zeta^3}{(3-\zeta)}\frac{\partial \ln s}{\partial \ln x}\left(\frac{\partial \ln s}{\partial \ln x} - 1\right) \\ \left. -2\left(\frac{a}{s}\right)^2\frac{\zeta^3}{(3-\zeta)}\frac{\partial^2 \ln s}{(\partial \ln x)^2}\right\}.\end{aligned} \quad (5.12)$$

Expression (5.12) supplements the system of relations (5.7)–(5.10) for the analysis of conditions of barrierless nucleation on soluble salt condensation nuclei.

6. APPROXIMATION OF THE SMALLNESS OF ADSORPTION

Let us simplify the solution to Eq. (5.7) assuming that strong inequality $|s|/\bar{a} \ll 1$ is fulfilled that, as was shown by numerical estimates using Eqs. (1.16) and (1.17), usually takes place even at relatively high concentrations of aqueous solutions of inorganic salts. Considering relations (1.16) and (1.17) and expanding

over small parameter $|s|/\bar{a} \ll 1$ in Eq. (5.7), with an accuracy to second-order terms, we find

$$\zeta = \frac{9\tilde{A}x\ln\tilde{B}x}{2\bar{a}}\left[1 - \frac{\tilde{A}x}{2\bar{a}}(4\ln\tilde{B}x + 11)\right]. \quad (6.1)$$

As is seen from Eqs. (1.16) and (1.17), strong inequality $|s|/\bar{a} \ll 1$ will be fulfilled, if condition

$$\left|\frac{\tilde{A}x\ln\tilde{B}x}{\bar{a}}\right| \ll 1 \quad (6.2)$$

is satisfied.

Substituting Eq. (6.1) into Eq. (5.10), we find, with the same accuracy, relations connecting ν_n and x in the point of maximum of condensate chemical potential

$$\nu_n = \left(\frac{2\bar{a}}{9}\right)^3 \frac{1}{ix^2}\left[1 - \frac{3\tilde{A}x}{2\bar{a}}(2\ln\tilde{B}x - 11)\right], \quad (6.3)$$

$$x = \left(\frac{2\bar{a}}{9}\right)^{3/2} \frac{1}{(i\nu_n)^{1/2}} \times\left[1 - \frac{\tilde{A}}{6}\left(\frac{2\bar{a}}{9i\nu_n}\right)^{1/2}\left(\ln\frac{8\tilde{B}^2\bar{a}^3}{729i\nu_n} - 11\right)\right]. \quad (6.4)$$

Substituting further Eqs. (6.1) and (6.4) into Eqs. (5.9) and (5.8), we find the dependence of ν_0 and maximum $b_\nu|_{\nu=\nu_0}$ of condensate chemical potential on ν_n with the accuracy of second-order terms

$$\nu_0 = \left(\frac{9i\nu_n}{2\bar{a}}\right)^{3/2}\left[1 - \frac{\tilde{A}}{6}\left(\frac{2\bar{a}}{9i\nu_n}\right)^{1/2}\left(2\ln\frac{8\tilde{B}^2\bar{a}^3}{729i\nu_n} + 11\right)\right], \quad (6.5)$$

$$b_\nu|_{\nu=\nu_0} = 2\left(\frac{2\bar{a}}{9}\right)^{3/2} \frac{1}{(i\nu_n)^{1/2}} \times\left[1 + \frac{\tilde{A}}{12}\left(\frac{2\bar{a}}{9i\nu_n}\right)^{1/2}\left(\ln\frac{8\tilde{B}^2\bar{a}^3}{729i\nu_n} + 4\right)\right]. \quad (6.6)$$

Let us discuss relation (6.6) in more detail. We take into account that number ν_n of salt molecules in a spherical condensation nucleus is related to its radius R_n by expression

$$R_n = \left(\frac{3v_n\nu_n}{4\pi}\right)^{1/3}, \quad (6.7)$$

where v_n is the volume per salt molecule in the nucleus. Passing from variable ν_n to variable R_n in the right-hand side of Eq. (6.6) and allowing for equality $b_{\text{th}} = b_\nu|_{\nu=\nu_0}$ and expression for the dimensionless chemical potential of vapor

$$b = \ln(1 + \xi), \quad (6.8)$$

as a function of nucleus supersaturation ξ, we write

$$\ln(1 + \xi_{\text{th}}) = 2\left(\frac{2\bar{a}}{9R_n}\right)^{3/2}\left(\frac{3v_n}{4\pi i}\right)^{1/2} \times\left[1 + \frac{\tilde{A}}{12}\left(\frac{\bar{a}v_n}{6\pi iR_n^3}\right)^{1/2}\left(\ln\frac{2\tilde{B}^2\bar{a}^3v_n}{243\pi iR_n^3} + 4\right)\right]. \quad (6.9)$$

Setting formally $\tilde{A} = 0$ in Eq. (5.9), we obtain $\bar{b}_{\text{th}} = \ln(1 + \bar{\xi}_{\text{th}}) = 2(2\bar{a}/9R_n)^{3/2}(3v_n/4\pi i)^{1/2}$ that represents Kohler's formula for the threshold vapor supersaturation upon the barrierless nucleation on soluble nuclei composed of inorganic salts with the disregard for adsorption.

Let us pass to the consideration of critical values of the chemical potential and vapor supersaturations at the barrier nucleation. Substituting Eqs. (1.16), (1.17), (6.1), and (6.4) into Eq. (5.12) with accuracy to second-order terms, we find

$$\left.\frac{\partial^2 b_\nu}{\partial\nu^2}\right|_{\nu=\nu_0} = -\frac{2}{3}\left(\frac{2\bar{a}}{9}\right)^{9/2} \frac{1}{(i\nu_n)^{7/2}} \times\left[1 + \frac{\tilde{A}}{3}\left(\frac{2\bar{a}}{9i\nu_n}\right)^{1/2}\left(2\ln\frac{8\tilde{B}^2\bar{a}^3}{729i\nu_n} + 9\right)\right]. \quad (6.10)$$

Let us express deviation ε of the critical value of vapor chemical potential from its threshold value as a function of height ΔF of activation barrier and ν_n. Using Eqs. (6.6) and (6.10), from Eq. (5.11), we obtain

$$\varepsilon = \bar{\varepsilon}\left[1 + \frac{\tilde{A}}{108}\left(\frac{2\bar{a}}{i\nu_n}\right)^{1/2}\left(5\ln\frac{8\tilde{B}^2\bar{a}^3}{729i\nu_n} + 24\right)\right], \quad (6.11)$$

where $\bar{\varepsilon} = (3^{1/3}/8)(2\Delta F/i\nu_n)^{2/3}$ represents the deviation of the critical value of vapor chemical potential at the same height ΔF of activation barrier in the absence of adsorption. Note that threshold value b_{th} corresponded to deviation ε, in view of Eq. (6.9), differs at given ν_n from threshold value $\bar{b}_{\text{th}}$ used to determine deviation $\bar{\varepsilon}$.

7. DOMAINS OF THE APPLICABILITY OF A THEORY AND DISCUSSION OF RESULTS

Let us set domains of the applicability of formulas (6.6) and (6.11) for the dependences of the threshold value of vapor chemical potential and critical vapor supersaturations on the number of molecules in the condensation nucleus. It is evident that these domains should be related to the conditions of the applicability of initial relation (5.1). In particular, according to relation (5.1), the condition of dilute solution

$$x \ll 1 \quad (7.1)$$

should be satisfied. As is seen from Eq. (6.4), condition (7.1) will be ensured in the principal order in the maximum of condensate chemical potential under the fulfillment of strong inequality

$$\nu_n^{1/2} \gg \frac{(2\bar{a})^{3/2}}{3^3 i^{1/2}}. \quad (7.2)$$

Note that, in view of Eq. (6.4), condition (7.1) of the applicability of expansion in powers of small adsorption is fulfilled when

$$\frac{\tilde{A}}{9}\left(\frac{2\bar{a}}{9i\nu_n}\right)^{1/2}\left|\ln\frac{8\tilde{B}^2\bar{a}^3}{729i\nu_n}\right| \ll 1 \quad (7.3)$$

a condition that, as well as inequality (7.2), restricts the admissible theoretical lower values of number ν_n of salt molecules in a droplet (and, in view of Eq. (6.7), radius R_n of salt particles). Inequalities (7.2) and (7.3) at $\nu_n \geq 250$ are almost equally satisfied for aqueous 1 : 1 electrolyte solution at the typical values of problem parameters considered in Section 3, i.e., at $i = 2$, $\bar{a} = 8.39$, $\tilde{A} = 1.34$, and $\tilde{B} = 0.047$ (for NaCl). As follows from Eq. (6.4), at $\nu_n \geq 250$, solution concentration x in a droplet corresponding to the maximum of condensate chemical potential satisfies inequality $x \leq 0.1$. At the same time, according to Eq. (6.5) and equality $R_0 = (3v\nu_0/4\pi)^{1/3}$, the droplet corresponding to the maximum of chemical potential has radius $R_0 \geq 50$ Å. According to Eq. (1.5), the Debye length $1/\kappa$ does not exceed 2 Å. As follows from Eq. (6.4), with an increase in ν_n, concentration x in droplets corresponding to the extremum of condensate chemical potential decreases in the principal order as $\nu_n^{-1/2}$. Then, according to Eq. (1.5), the Debye length increases with ν_n as $\nu_n^{1/4}$. In this case, according to Eq. (6.5), number ν_0 of condensate molecules in a droplet increases as $\nu_n^{3/2}$; correspondingly, droplet radius R_0 increases as $\nu_n^{1/2}$, i.e., faster than the Debye length. All this confirms the assumption of the relative smallness of Debye length made in Section 4 for droplets that are of interest to us. Note that, in this case, the assumption that the Debye length is independent of the distance form the interface used in Section 1 turned out to be at the limit of its applicability. Thus, results obtained near $\nu_n \approx 250$ should be considered as received at the limit of theory applicability.

Note that, at $250 \leq \nu_n \leq 3000$ and according to Eq. (6.4) at $0.1 \geq x \geq 0.03$, strong inequality $\kappa d \ll 1$ can be violated or fulfilled at the limiting applicability. As was already mentioned in Section 3, relations of (1.16) and (1.17) type used in Sections 4 and 5 are applicable even at higher solution concentrations that those allowed by inequality $\kappa d \ll 1$.

Relations (5.1) and (5.2) also require the fulfillment of the condition of complete dissolution of condensation nucleus in a droplet in the point of largest maximum of condensate chemical potential, which has the following form [23]:

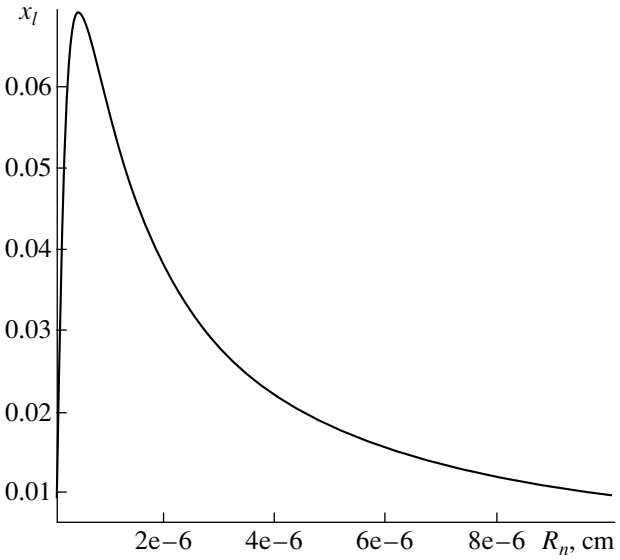


Fig. 7. Dependence of the limiting value x_l of saturation concentration for the bulk solution determined by the right-hand side of inequality (7.4) on the radius of condensation nucleus composed of NaCl.

$$x_\infty > \frac{2\bar{\sigma}v}{R_n k_B T}\exp\left\{-\frac{2\sigma_n v_n}{R_n k_B T}\right\}\left(1-\left(\frac{4\bar{\sigma}v_n}{R_n k_B T}\right)^{1/2}\right). \quad (7.4)$$

Here, x_∞ is the saturation concentration for the solution of the substance comprising condensation nucleus in the condensate (salt solubility), $\kappa d \ll 1$ σ_n is surface tension of the substance comprising condensation nucleus in a solid state at the boundary with the solution in the condensate.

Figure 7 presents the dependence of the right-hand side of Eq. (7.4) on the radius of condensation nucleus at typical values of the parameters of solution and nucleus ($T = 300$ K, $\bar{\sigma} = 73$ dyne/cm, $v = 3 \times 10^{-23}$ cm^3, $\sigma_n = 200$ dyne/cm, and $v_n = 4.5 \times 10^{-23}$ cm^3). It is seen that the assumption of the complete dissolution of nucleus in a droplet in the point of largest maximum of condensate chemical potential is justified throughout the range of discussed sizes of condensation nuclei composed of salts (strong electrolytes), provided that salt solubility satisfies inequality $x_\infty > 0.07$. For example, this is true for the case of NaCl, Na_2SO_4, and $MgCl_2$ particles.

Note that, for droplets larger than those corresponding to the maximum of condensate chemical potential, conditions of complete dissolution and dilute solutions in a droplet will be fulfilled even stronger.

Figure 8 illustrates the dependence of the threshold (for the barrierless nucleation) value of vapor chemical potential $b_{th} = b_\nu|_{\nu = \nu_0}$ on the size of condensation nuclei composed of NaCl plotted by formula (6.6) (curve *1*). Figure 8 shows also curve *2* that corresponds

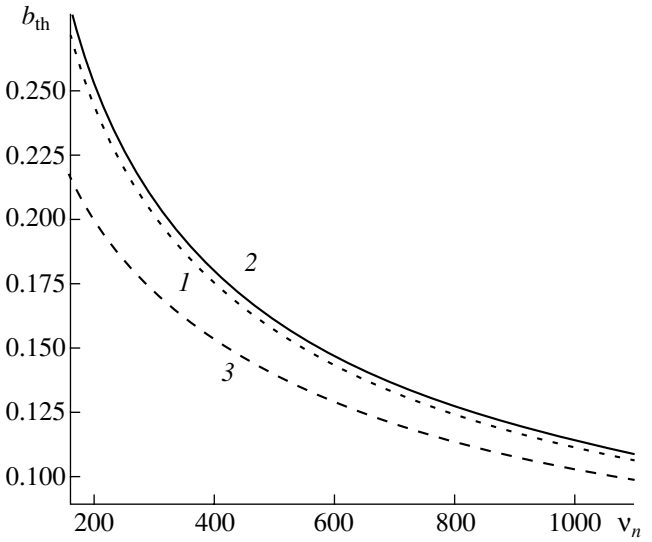


Fig. 8. Dependences of the threshold value of vapor chemical potential on the size of condensation nucleus composed of NaCl calculated (*1*) using Eq. (6.6), (*2*) by Kohler's formula, and (*3*) in the approximation of Henry's law.

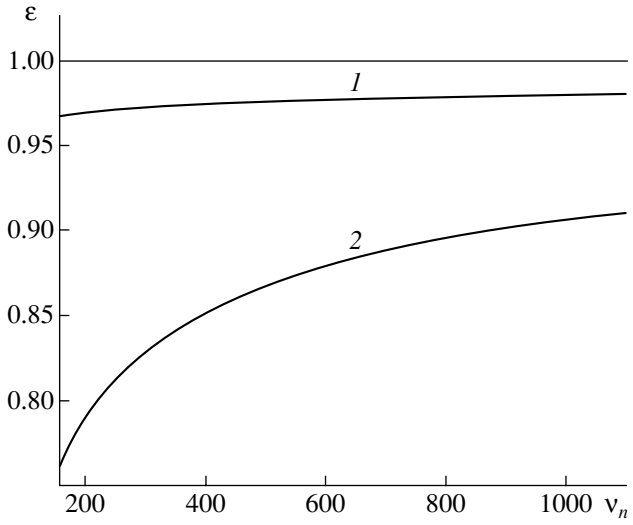


Fig. 9. Relative deviation of the critical value of vapor chemical potential below its threshold value as a function of the size of condensation nucleus composed of NaCl calculated (*1*) using Eq. (6.11) and (*2*) in the approximation of Henry's law.

to Kohler's formula disregarding the adsorption of dissolved substance on the droplet surface and curve *3* plotted under the assumption of the validity of Henry adsorption law (relevant dependences have the form of $(b_\nu|_{\nu=\nu_0})_{\mathcal{H}} = 4(\bar{a}/9)^{3/2}\nu_n^{-1/2}[1 + (1/18\mathcal{H})\sqrt{\bar{a}/\nu_n}]$, $\varepsilon_{\mathcal{H}} = \bar{\varepsilon}[1 + (5/54\mathcal{H})\sqrt{\bar{a}/\nu_n}]$ [25], and $\mathcal{H}_{NaCl} = -0.096$ [14]). It is seen that the allowance for ion adsorption on the droplet surface leads to a decrease in the threshold value of vapor chemical potential by several percents. The use of Henry's law gives a significant error that exceeds about threefold the deviation in case of total allowance for adsorption. Differences between curves actually disappear with an increase in the size of condensation nuclei.

Figure 9 shows the dependences of relative deviation $\varepsilon/\bar{\varepsilon}$ of the critical value of vapor chemical potential upon the barrier nucleation from the threshold value upon the barrierless nucleation on the size of condensation nuclei composed of NaCl: the dependence plotted by formula (6.11) and that corresponding to the Henry adsorption law. In is seen that the dependence corresponding to the Henry law also leads to large relative error.

Figures 10 and 11 present the dependences of $b_{th} = b_\nu|_{\nu=\nu_0}$ and $\varepsilon/\bar{\varepsilon}$ on the size of condensation nuclei for strong 2 : 1 and 1 : 2 electrolytes, Na_2SO_4 and $MgCl_2$, respectively. It is seen that the pattern of relative corrections to the threshold value of vapor chemical potential is the same as for the relative deviations of the surface tension of Na_2SO_4 and $MgCl_2$ solutions from the surface tension of pure water (see Fig. 5). These deviations are more distinctly exhibited in case of $MgCl_2$ and can be as high as 10%. According to Fig. 11, differences in the deviations of critical values of vapor chemical potential in the kinetics of barrier nucleation on nuclei composed of $MgCl_2$ can be even more distinct. This can lead to the experimentally detected differences in nucleation rates on condensation nuclei of the same size, but composed of different electrolyte salts.

Note that, in practice, we deal with the dependences of thermodynamic parameters on the nucleus radius

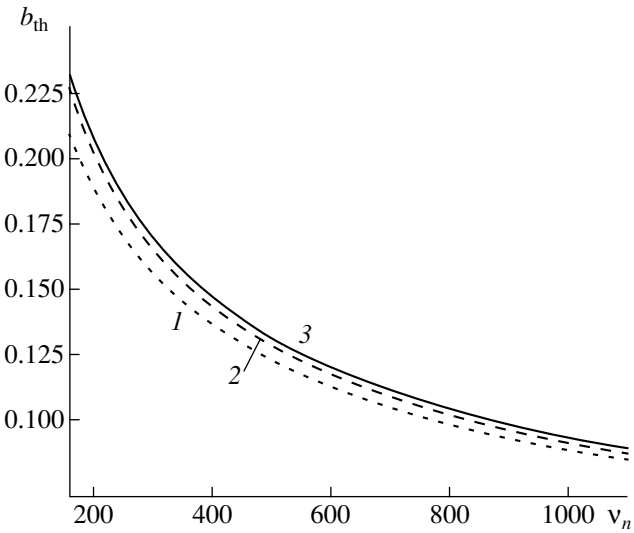


Fig. 10. Dependences of the threshold value of vapor chemical potential on the size of condensation nucleus composed of (*1*) $MgCl_2$ and (*2*) Na_2SO_4 calculated using Eq. (6.6). Curve *3* is analogous dependence calculated for 2 : 1 electrolyte with the disregard for adsorption.

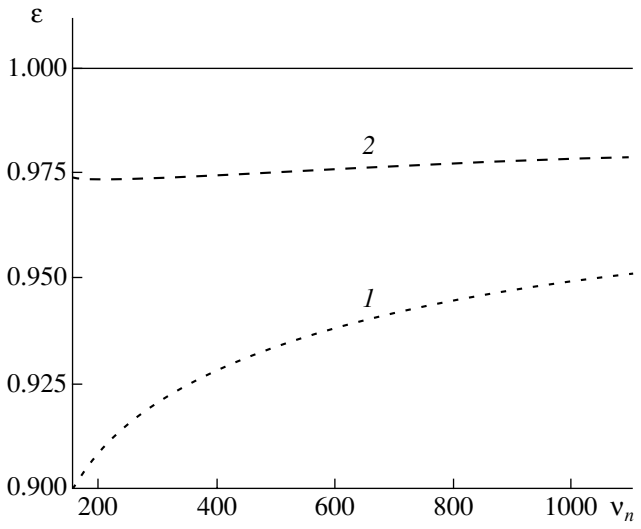


Fig. 11. Relative deviation of the critical value of vapor chemical potential below the threshold value as a function of the size of condensation nuclei composed of (*1*) $MgCl_2$ and (*2*) Na_2SO_4.

rather on the number of molecules in condensation nucleus. In this situation, different salts exhibit their specificity, above all, via the differences in the density of substance comprising their particles that agrees with the results obtained in [4].

ACKNOWLEDGMENTS

This work was supported by the Universities of Russia–Fundamental Research Program, project no. UR.01.01.042.

REFERENCES

1. Kohler, H., *Trans. Faraday Soc.*, 1936, vol. 32, p. 1152.
2. Dufour, L. and Defay, R., *Thermodynamics of Clouds,* New York: Academic, 1963.
3. Laktionov, A.G., *Ravnovesnaya geterogennaya kondensatsiya* (Equilibrium Heterogeneous Condensation), Leningrad: Gidrometeoizdat, 1988.
4. Herber, H.E., Hoppel, W.A., and Wojciechovski, T.A., *J. Atmos. Sci.*, 1977, vol. 34, p. 1836.
5. Wagner, C., *Phys. Z.*, 1924, vol. 25, p. 474.
6. Onsager, L. and Samaras, N.N.T., *J. Chem. Phys.*, 1934, vol. 2, p. 527.
7. Buff, F.P. and Stillinger, F.H., *J. Chem. Phys.*, 1956, vol. 25, p. 312.
8. Groenewald, J., *J. Chem. Phys.*, 1997, vol. 107, p. 9668.
9. Levin, Y., *J. Chem. Phys.*, 2000, vol. 113, p. 9722.
10. Randles, J.E.B., in *Advances in Electrochemistry and Electrochemical Engineering*, Ed. by Delahay, P. and Tobias, C.W., New York: Wiley, 1963, vol. 3, p. 1.
11. Aveyard, R. and Saleem, S.M., *J. Chem. Soc., Faraday Trans. 1,* 1976, vol. 72, p. 1609.
12. Weissenborn, P.K. and Pugh, R.J., *J. Colloid Interface Sci.*, 1996, vol. 184, p. 550.
13. Ninham, B.W., Kurihara, K., and Vinogradova, O.I., *Colloids Surf., A*, 1997, vols. 123–124, p. 7.
14. Ninham, B.W. and Yaminsky, V., *Langmuir*, 1997, vol. 13, p. 2097.
15. Böstrom, M., Williams, D.R.M., and Ninham, B.W., *Langmuir*, 2001, vol. 17, p. 4475.
16. Manciu, M. and Ruckenstein, E., *Adv. Colloid Interface Sci.*, 2002, vol. 105, p. 63.
17. Karraker, K.A. and Radke, C.J., *Adv. Colloid Interface Sci.*, 2002, vol. 96, p. 231.
18. Kunz, W., Lo Nostro, P., and Ninham, B.W., *Curr. Opin. Colloid Interface Sci.*, 2004, vol. 9, p. 1.
19. Jungwirth, P. and Tobias, D.J., *J. Phys. Chem., B,* 2002, vol. 106, p. 6361.
20. Dang, L.X., *J. Phys. Chem., B*, 2002, vol. 106, p. 10 388.
21. Mucha, M., Frigato, T., Levering, L., *et al.*, *J. Phys. Chem., B*, 2005, vol. 109, p. 7617.
22. Gopalakrishnan, S., Jungwirth, P., Tobias, D.J., and Allen, H.C., *J. Phys. Chem., B*, 2005, vol. 109, p. 8861.
23. Schmutzer, E., *Z. Phys. Chem.* (Munich), 1955, vol. 204, p. 131.
24. Ho, C.-H., Tsao, H.-K., and Sheng, Y.-J., *J. Chem. Phys.,* 2003, vol. 119, p. 2369.
25. Shchekin, A.K., Kuni, F.M., Yakovenko, T.M., and Rusanov, A.I., *Kolloidn. Zh.*, 1995, vol. 57, p. 99.
26. Kuni, F.M., Shchekin, A.K., and Grinin, A.P., *Usp. Fiz. Nauk*, 2001, vol. 171, p. 345.